ECCOMAS Congress 2016
VII European Congress on Computational Methods in Applied Sciences and Engineering
M. Papadrakakis, V. Papadopoulos, G. Stefanou, V. Plevris (eds.)
Crete Island, Greece, 5–10 June 2016

THE VIRTUAL ELEMENT METHOD FOR DISCRETE FRACTURE NETWORK FLOW AND TRANSPORT SIMULATIONS

Matías Fernando Benedetto, Stefano Berrone, Andrea Borio, Sandra Pieraccini, and Stefano Scialo

Politecnico di Torino
Corso Duca degli Abruzzi, 24 – 10129, Torino (TO), Italy
e-mail: {matias.benedetto,stefano.berrone,andrea.borio,sandra.pieraccini,stefano.scialo}@polito.it

Keywords: Discrete Fracture Network, Virtual Element Method, Underground flow, Fractured media.

Abstract. *We discuss several issues concerning the application of the Virtual Element Method (VEM) to the flow in fractured media modeled by the Discrete Fracture Network (DFN) model. Due to the stochastic nature of the computational domains, several geometrical complexities make the computations very challenging. The geometrical flexibility provided by the Virtual Element Method can be exploited to mutually couple local problems, either by resorting to a Mortar approach, or by allowing for the global conformity of the local meshes, while keeping the computational cost under control. We describe these two approaches in detail and we test them on a realistic test case, showing the viability of the two approaches.*

1 Introduction

Subsurface fluid flow has applications in a wide range of fields, including e.g. oil/gas recovery, gas storage, pollutant percolation, water resources monitoring. Underground fluid flow in fractured media is a heterogeneous multi-scale phenomenon that involves complex geological configurations; a possible approach for modeling the phenomenon is given by Discrete Fracture Networks (DFNs), which are complex sets of polygonal intersecting fractures randomly generated from known distributions for geometrical features (such as orientation in the three dimensional space, position, dimensions) and hydro-geological properties. Geological fractured media are therefore characterized by a very challenging geometrical complexity, which is one of the major difficulties to be tackled when performing flow simulations.

In this work we recall some results concerning the application of the Virtual Element Method [4, 3, 2] to the steady state simulation of the flow in DFNs [1, 22, 27, 30, 24, 32, 23, 15, 16, 17, 18, 19, 9, 10, 8, 13]. In this approach we can exploit the flexibility of VEM in order to tackle the geometrical complexity. Indeed, a crucial issue in DFN flow simulations is the need to provide on each fracture a good quality mesh [24, 20, 29, 30] on any randomly generated configuration. Namely, if classical triangular or quadrilateral meshes on the fractures are required to be conforming to the traces (fracture intersections), and also conforming each other, the meshing process for each fracture is not independent of the others, thus yielding in practice a quite demanding computational effort for the mesh generation process. In some cases, the meshing process may even result infeasible so that some authors propose to modify the DFN removing problematic fractures [24].

Here, the VEM will be used within several possible approaches to the problem: in conjunction with a totally conforming polygonal mesh [10] and with a Mortar approach [8]. Indeed, taking advantage from the great flexibility of VEM in allowing the use of rather general polygonal mesh elements, a suitable mesh for representing the solution and imposing matching conditions between the solutions on different fractures can be easily obtained, starting from an arbitrary triangular mesh independently built on each fracture, and independent of the trace disposition. Robustness and efficiency of the approach are of great importance also in the framework of Uncertainty Quantification analysis applied to DFNs, see [14].

The paper is organized as follows: after introducing some notation about the DFNs in Section 2, we describe the more common geometrical complexities present in DFNs flow simulations in Subsection 2.1. The problem considered and the formulation used are described in Section 3. Section 4 is devoted to discuss the VEM formulation and some issues concerning its implementation. Subsection 4.3 recalls the elements of a hybrid mortar approach to the matching conditions, whereas Subsection 4.4 recalls the basic ideas of a globally conforming approach. Finally, we propose in Section 5 some numerical results obtained with the two approaches.

2 Discrete Fracture Networks

A DFN is a possible model for a fractured medium in which the surrounding rock matrix can be assumed to be impervious. In a DFN, fractures in the underground medium are represented as bi-dimensional open polygons. The intersections between fractures are called *traces*, and we assume, for the sake of simplicity, that precisely two fractures meet at each trace. For a DFN Ω, we will indicate by F_i the generic fracture, with $i \in \mathcal{I} = \{1, \dots, N\}$, while its boundary will be $\partial\Omega = \cup_{i\in\mathcal{I}}\partial F_i$. Traces will be denoted by Γ_m, with $m \in \mathcal{M} = \{1, \dots, M\}$. Without loss of generality, we assume that the set $\bar{\Omega}$ is connected. Finally, we introduce the following notation:

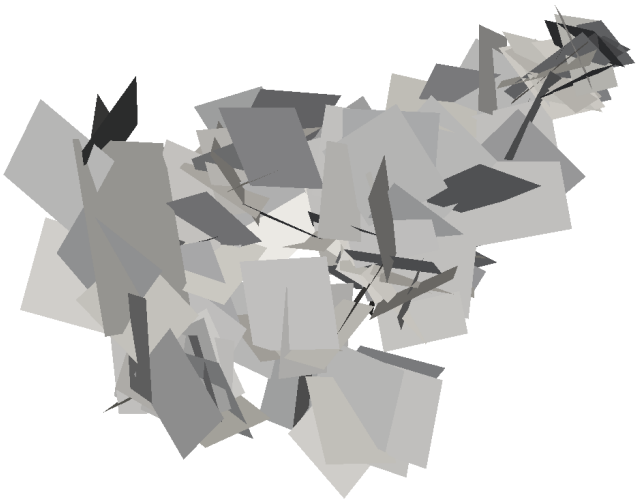

Figure 1: DFN with 134 fractures

- $\forall i \in \mathcal{I}$, let $\mathcal{M}_i \subset \mathcal{M}$ be the subset of trace indices corresponding to traces lying on F_i; each subset $\mathcal{M}_i$ is assumed to be ordered, and we will denote by $\mathcal{M}_i(k)$ the k-th index of a trace in $\mathcal{M}_i$;
- $\forall m \in \mathcal{M}$, let $\mathcal{I}_m = (i, j)$ be the ordered couple of indices such that $\Gamma_m = F_i \cap F_j$, with $i < j$;
- for each $i \in \mathcal{I}$ and each $m \in \mathcal{M}_i$, we fix a unit vector $\hat{n}^i_m$ normal to Γ_m on F_i.

2.1 Geometrical issues

When dealing with DFN flow simulations, the greatest obstacle is to devise a robust and efficient meshing process, while enforcing some kind of conformity of the mesh polygons to the traces. This can be required locally on each fracture, or globally, asking that polygons on different fractures meeting on the same trace share either one point or a whole side. These constraints can make the meshing process infeasible using traditional simplicial elements, because traces may intersect with very small angles, may have very different lengths or can be very close to each other without intersections. To illustrate how common are problematic configurations, let us consider a quite simple, although realistic, DFN containing 134 fractures; the DFN is displayed in Figure 1. Even though fractures in this DFN are of comparable size (see Figure 2a) the trace lengths span several orders of magnitude (Figure 2b), thus creating problems when mesh edges are required either to lie entirely on traces or have an intersection with them with a null measure. Furthermore, in Figure 3a we show the global distribution of angles between intersecting traces, while Figure 3b shows that a considerable amount of them is very small, making it very hard to build good quality triangular elements close to the corresponding intersections. Finally, another geometrical issue which is worth to analyze is the presence of very close and non – intersecting traces. In Figure 4 we see that there is a significant amount of them, which would yield very small elements, in case a regular triangulation is built.

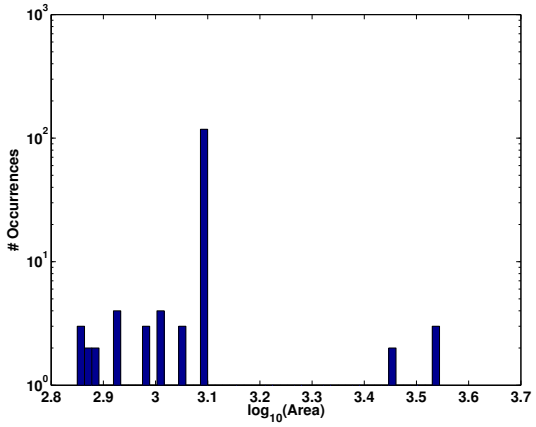

(a) Distribution of fracture areas.

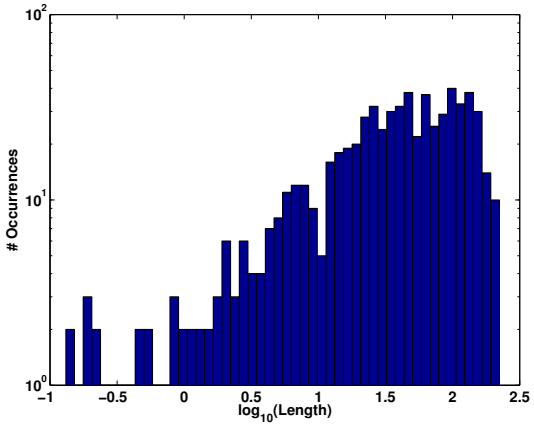

(b) Distribution of trace lengths.

Figure 2: Distribution of fracture areas and traces lengths of the DFN in Figure 1.

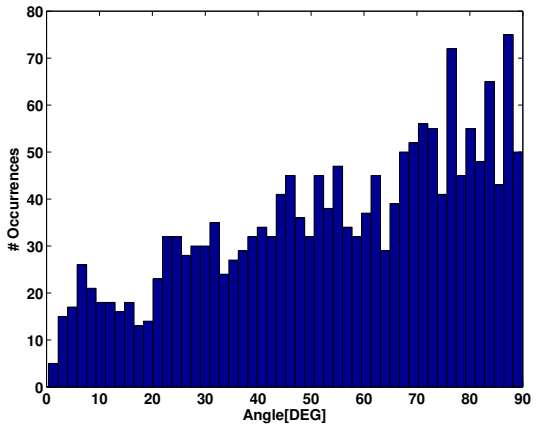

(a) Full distribution.

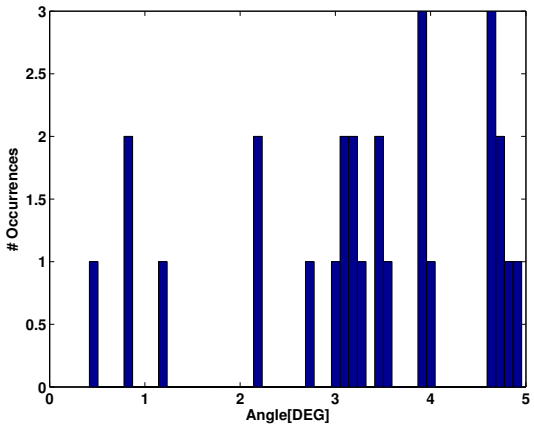

(b) Occurrences of very small angles.

Figure 3: Distribution of angles between traces for the DFN in Figure 1.

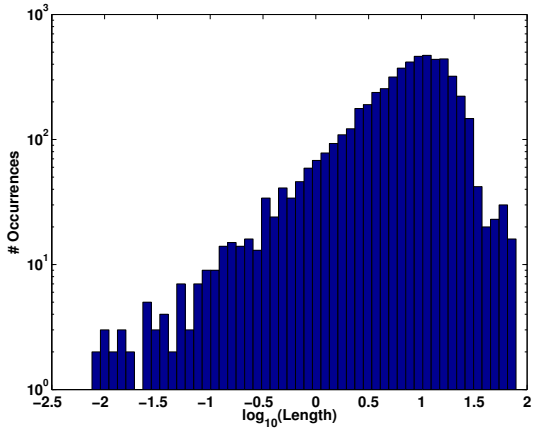

(a) Full distribution.

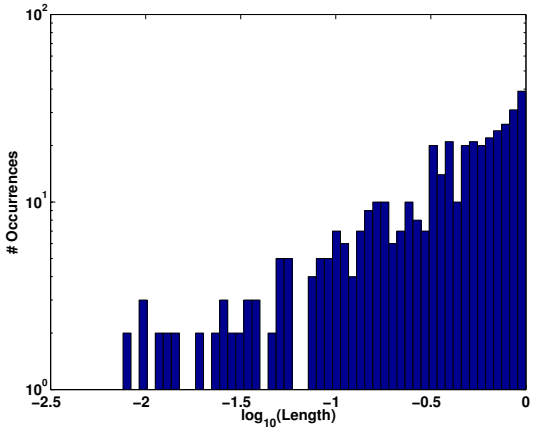

(b) Occurrences of very small distances.

Figure 4: Distribution of distance between non intersecting traces for the DFN in Figure 1

3 Problem formulation

Given an open bounded domain ω, let $(\cdot,\cdot)_\omega$ and $\|\cdot\|_\omega$ denote the $\mathrm{L}^2(\omega)$ scalar product and norm, respectively, and $(\cdot,\cdot)_{\alpha,\omega}$ and $\|\cdot\|_{\alpha,\omega}$ denote the $\mathrm{H}^\alpha(\omega)$ scalar product and norm, respectively. In general, a subscript i will denote the restriction of a function to the fracture F_i.

For any segment $\sigma \subset F_i$, $i \in \mathcal{I}$, we introduce the trace operator $\gamma_\sigma \colon \mathrm{H}^1(F_i) \to \mathrm{H}^{\frac{1}{2}}(\sigma)$ and the notation

$$\langle \mu, \beta \rangle_\sigma := {}_{\mathrm{H}^{-\frac{1}{2}}(\sigma)}\langle \mu, \beta \rangle_{\mathrm{H}^{\frac{1}{2}}(\sigma)}, \quad \forall \mu \in \mathrm{H}^{-\frac{1}{2}}(\sigma), \beta \in \mathrm{H}^{\frac{1}{2}}(\sigma),$$

to denote the duality product between $\mathrm{H}^{-\frac{1}{2}}(\sigma)$ and $\mathrm{H}^{\frac{1}{2}}(\sigma)$. Let $v \in \mathrm{H}^1(F_i)$, in order to simplify the notation, it is convenient to introduce the vectors $\gamma_{\mathcal{M}_i}(v)$, $\forall i \in \mathcal{I}$, the k-th element of $\gamma_{\mathcal{M}_i}(v)$ being $\gamma_{\Gamma_{\mathcal{M}_i(k)}}(v)$. Furthermore, we introduce the jump across a trace Γ_m as

$$[\![v]\!]_{\Gamma_m} := \gamma_{\Gamma_m}(v_i) - \gamma_{\Gamma_m}(v_j), \quad \text{if } \mathcal{I}_m = (i,j),$$

and we introduce the symbols $[\![v]\!]_{\mathcal{M}}$ and $[\![v]\!]_{\mathcal{M}_i}$ to denote the vectors of jumps of v across all traces in the network, and across traces on F_i, respectively. With the same purpose, $\forall i \in \mathcal{I}$, we introduce the notation

$$\langle \mu, \beta \rangle_{\mathcal{M}_i} := \sum_{m \in \mathcal{M}_i} \langle \mu_m, \beta_m \rangle_{\Gamma_m}, \ \forall \mu \in \prod_{m \in \mathcal{M}_i} \mathrm{H}^{-\frac{1}{2}}(\Gamma_m), \beta \in \prod_{m \in \mathcal{M}_i} \mathrm{H}^{\frac{1}{2}}(\Gamma_m).$$

Finally, for any $\beta, \lambda \in \prod_{m \in \mathcal{M}_i} \mathrm{H}^{\frac{1}{2}}(\Gamma_m)$ we denote

$$(\beta, \lambda)_{\mathcal{M}_i} := \sum_{m \in \mathcal{M}_i} (\beta, \lambda)_{\Gamma_m}.$$

We are interested in computing the hydraulic head $h = \pi/(\rho g) + z$, where π is the fluid pressure, g the gravitational acceleration, ρ the fluid density and z the elevation. The hydraulic head, on each fracture F_i, is modeled by means of the Darcy law as follows.

Let K_i denote the transmissivity on F_i, which we assume to be constant, and $f_i = f_i(x)$ denote the source term on F_i; notice that both K_i and f_i are functions of the local tangential coordinate system. Let $\Gamma^D \subseteq \partial\Omega$ be the Dirichlet boundary, and let h^D be the Dirichlet boundary condition defined on Γ^D. We define the functional spaces:

$$\begin{aligned}
V_i &:= \left\{ v \in \mathrm{H}^1(F_i) : \gamma_{\Gamma^D}(v) = 0 \right\} && \forall i \in \mathcal{I}, \\
V_i^D &:= \left\{ v \in \mathrm{H}^1(F_i) : \gamma_{\Gamma^D}(v) = h_i^D \right\} && \forall i \in \mathcal{I}, \\
V &:= \left\{ v \colon v_i \in V_i \quad \forall i \in \mathcal{I} \right\}, \\
V^D &:= \left\{ v \colon v_i \in V_i^D \quad \forall i \in \mathcal{I} \right\}.
\end{aligned}$$

On each fracture F_i, $i \in \mathcal{I}$, we want to find $h_i \in V_i^D$ such that, $\forall v_i \in V_i$,

$$a_i(h_i, v_i) := (\mathrm{K}_i \nabla h_i, \nabla v_i)_{F_i} = (f_i, v_i)_{F_i} + \left\langle h_i^N, \gamma^i_{\Gamma_i^N}(v_i) \right\rangle_{\Gamma_i^N} + \left\langle \left[\!\left[\frac{\partial h_i}{\partial \hat{n}_{\mathcal{M}_i}} \right]\!\right]_{\mathcal{M}_i}, \gamma_{\mathcal{M}_i}(v_i) \right\rangle_{\mathcal{M}_i} \tag{1}$$

where $\left[\!\left[\frac{\partial h_i}{\partial \hat{n}^i_m} \right]\!\right]_{\Gamma_m}$ is the jump of the co-normal derivative $\frac{\partial h_i}{\partial \hat{n}^i_m} = \mathrm{K}_i \nabla h_i \cdot \hat{n}^i_m$ along $\hat{n}^i_m$; furthermore, $\Gamma_i^N \subseteq \partial F_i$ is the Neumann boundary on F_i and $h_i^N \in \mathrm{H}^{-\frac{1}{2}}\left(\Gamma_i^N\right)$ is the Neumann

boundary condition. For future reference, we set $\Gamma^N = \cup_{i\in\mathcal{I}}\Gamma_i^N \subset \partial\Omega$ and define h^N such that h_i^N is the restriction of h^N to F_i. We couple the problems on each fracture by imposing the continuity of the solution and balance of incoming and outgoing fluxes at each trace: $\forall m \in \mathcal{M}$, with $\mathcal{I}_m = (i,j)$, we have

$$\begin{aligned}\left[\!\left[h\right]\!\right]_{\Gamma_m} &= \gamma_{\Gamma_m}(h_i) - \gamma_{\Gamma_m}(h_j) = 0,\\ \left[\!\left[\frac{\partial h_i}{\partial \hat{n}_m^i}\right]\!\right]_{\Gamma_m} &+ \left[\!\left[\frac{\partial h_j}{\partial \hat{n}_m^j}\right]\!\right]_{\Gamma_m} = 0.\end{aligned} \tag{2}$$

3.1 Saddle point formulation of the DFN problem

The DFN problem (1)-(2) can be easily re-formulated as a saddle point problem. To this aim, let us first define, for each trace $m \in \mathcal{M}$, and recalling that $\mathcal{I}_m = (i,j)$, the function s_{Γ_m} such that:

$$s_{\Gamma_m}(i) = 1, \quad s_{\Gamma_m}(j) = 0,$$

and, for each fracture, a bilinear form $b_i\colon M_i := \prod_{m\in\mathcal{M}_i} \mathrm{H}^{-\frac{1}{2}}(\Gamma_m) \times V_i \to \mathbb{R}$ defined by

$$b_i(v,\psi) := \sum_{m\in\mathcal{M}_i} (-1)^{s_{\Gamma_m}(i)} \left\langle \psi_m, \gamma_{\Gamma_m}(v_i)\right\rangle_{\Gamma_m}.$$

Moreover, let us define

$$b(v,\psi) := \sum_{i\in\mathcal{I}} b_i(v,\psi) = \sum_{m\in\mathcal{M}} \left\langle \psi_m, \left[\!\left[v\right]\!\right]_{\Gamma_m}\right\rangle_{\Gamma_m}.$$

These bilinear forms are used in the definition of the functional $\mathcal{F}\colon V\times M := \prod_{m\in\mathcal{M}} \mathrm{H}^{-\frac{1}{2}}(\Gamma_m)$, given as a sum of contributions from the different fractures:

$$\begin{aligned}\mathcal{F}(v,\mu) := \sum_{i\in\mathcal{I}} \frac{1}{2}(\mathrm{K}_i\nabla v_i, \nabla v_i)_{F_i} - (f_i, v_i)_{F_i} - \left\langle h_i^N, \gamma_{\Gamma_i^N}^i(v_i)\right\rangle_{\Gamma_i^N}\\ + \left(\nabla\mathcal{R}_i\left(h_i^D\right), \nabla v_i\right)_{F_i} + b_i(v,\mu) + b_i\left(\mathcal{R}_i\left(h_i^D\right),\mu\right),\end{aligned}$$

where $\mathcal{R}_i$ is the lifting operator from $\mathrm{H}^{\frac{1}{2}}(F_i)$ to $\mathrm{H}^1(F_i)$, $i \in \mathcal{I}$.

The solution $(h,\lambda) \in V^D \times M$ such that $h_i = h_i^0 + \mathcal{R}_i\left(h^D\right)$, $h_i^0 \in V_i$, $i \in \mathcal{I}$ and

$$\mathcal{F}\left(h^0,\lambda\right) = \min_{v\in V}\max_{\psi\in M} \mathcal{F}(v,\psi), \tag{3}$$

is equivalent to the unique solution to the problem: $h = h^0 + \mathcal{R}\left(h^D\right)$, with $h^0 \in V$ and $\lambda \in M$ such that,

$$\begin{cases} a(h^0,v) + b(v,\lambda) = (f,v) + \left(h^N,v\right)_{\Gamma^N} - a(\mathcal{R}\left(h^D\right),v) & \forall v \in V,\\ b(h^0,\psi) = -b\left(\mathcal{R}\left(h^D\right),\psi\right) & \forall \psi \in M,\end{cases} \tag{4}$$

that provides the solution to the problem (1)-(2), as it can be proven following classical arguments (see e.g. [31]). Moreover, we have

$$\lambda_m = \left[\!\left[\frac{\partial h_i}{\partial \hat{n}_m^i}\right]\!\right]_{\Gamma_m} = -\left[\!\left[\frac{\partial h_j}{\partial \hat{n}_m^j}\right]\!\right]_{\Gamma_m},$$

with $\mathcal{I}_m = (i,j)$.

4 The discrete DFN problem

First introduced in [4] and extended in [5, 6, 3, 21, 2, 26], the Virtual Element Method allows the use of quite general non-degenerate and star-shaped polygons to mesh the spatial domain, even including the possibility of straight angles. In the present framework, we take advantage from this flexibility to easily build a mesh which, on each fracture, is locally or globally conforming to the traces. In the following of this section, we review the use of VEM, focusing on the framework of DFN simuations.

4.1 Construction of the mesh

Let a fracture F_i be fixed. To obtain a locally conforming mesh, we first introduce on F_i a triangular mesh built independently of trace positions; the triangles are then cut into polygons by the traces, possibly prolonging the trace segment up to the nearest mesh edge if it happens to end in the interior of a triangle. Note that in this latter case the trace tip is kept as a node of the discretization and the trace is not modified, a new node is created at the intersection between the prolongation of the trace segment and the mesh edge, and therefore two edges are created, with a $180°$ angle between them. Let $\mathcal{T}_{\delta i}^{\text{lc}}$ be the resulting local mesh. We refer to Figure 5 for a possible mesh configuration and to Figure 6a for a locally conforming mesh on a fracture. Let $\mathcal{T}_{\delta}^{\text{lc}} = \cup_{i\in\mathcal{I}}\mathcal{T}_{\delta i}^{\text{lc}}$. We will use the symbols $\mathcal{E}_{\delta i}^{\text{lc}}$ and $\mathcal{V}_{\delta i}^{\text{lc}}$ to denote the sets of edges and vertices on fracture F_i, respectively, and define the sets of the mesh edges and vertices of the whole DFN as $\mathcal{E}_{\delta}^{\text{lc}} = \cup_{i\in\mathcal{I}}\mathcal{E}_{\delta i}^{\text{lc}}$, $\mathcal{V}_{\delta}^{\text{lc}} = \cup_{i\in\mathcal{I}}\mathcal{V}_{\delta i}^{\text{lc}}$, respectively. The mesh built in this way can be used to couple VEM discretizations on each fracture with a Mortar approach, as described in subsection 4.3.

Another possible meshing process, that aims at building a globally conforming mesh $\mathcal{T}_{\delta}^{\text{gc}}$, can be devised as follows, starting from the above described mesh $\mathcal{T}_{\delta}^{\text{lc}}$. Let us consider an arbitrary trace Γ_m, with $m \in \mathcal{M}$ and $\mathcal{I}_m = (i, j)$. Then, we add to $\mathcal{T}_{\delta i}^{\text{lc}}$ the nodes generated by $\mathcal{T}_{\delta j}^{\text{lc}}$ on Γ_m, and viceversa. Some polygons belonging to mesh $\mathcal{T}_{\delta i}^{\text{lc}}$ ($\mathcal{T}_{\delta j}^{\text{lc}}$, respectively) having an edge lying on Γ_m, will possibly have such edges split by the new nodes, the new edges forming a straight angle at their intersection. Again, we refer the reader to Figure 5 for a visualization of a rather intricate trace configuration and to Figure 6b for a resulting globally conforming mesh on a fracture. All sets of geometrical objects relative to this globally conforming mesh will have a superscript "gc" in the following. This spatial discretization will be used in subsection 4.4 to allow the construction of VEM spaces containing globally continuous functions.

To further illustrate this process, we show in Figure 6 a possible situation in which the number of nodes on traces in $\mathcal{T}_{\delta}^{\text{gc}}$ is larger than the number of nodes in $\mathcal{T}_{\delta}^{\text{lc}}$. In the two subfigures, traces are drawn in red: as we can see the globally conforming mesh in Figure 6b presents some nodes that do not correspond to intersections between polygons and traces, but are induced by polygons on another fracture that generate the same trace. These nodes are not treated as hanging nodes, but as vertices of a polygon whose edges meeting there form a flat angle. The locally conforming mesh, instead, uses as nodes only the intersections between local polygons and traces. Finally, notice that in both cases the trace tip is added as a node.

Remark. All the elements created with the above procedures are convex.

4.2 The VEM setting

Let us now briefly sketch the main ideas at the basis of the use of the VEM in the context of flow simulations in complex networks of fractures, referring to the specific literature (see e.g. [4, 6, 2]) for a deeper insight about the method.

Let $k \in \mathbb{N}$ be a fixed polynomial degree, corresponding to the desired polynomial accuracy

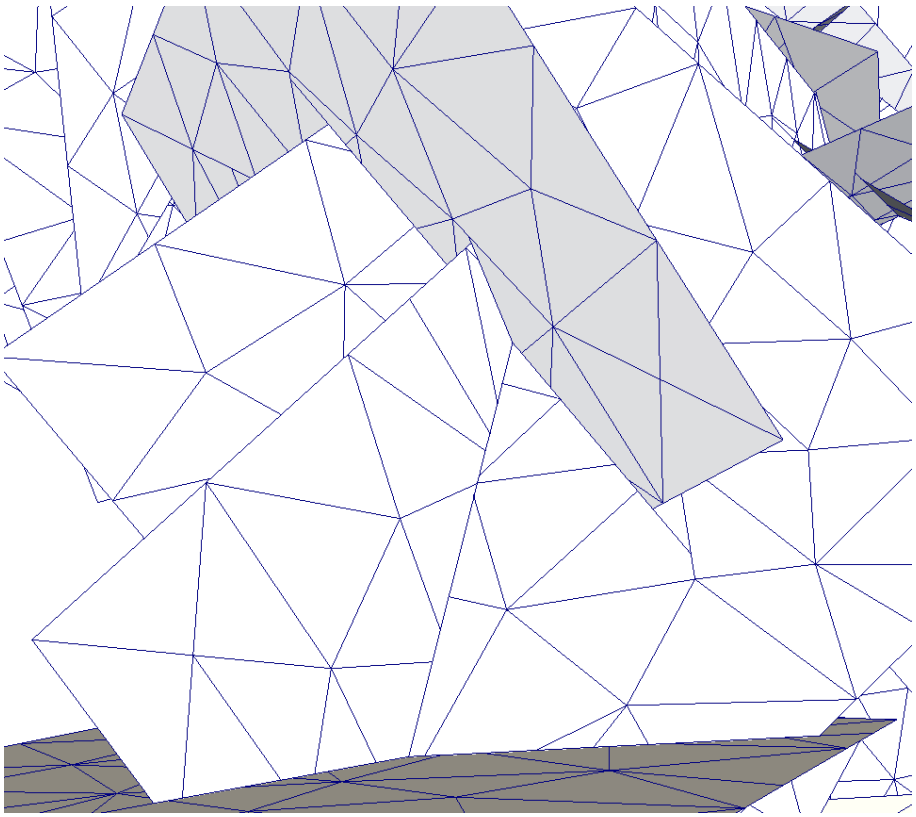

Figure 5: A detail of the mesh around traces on the DFN in Figure 1

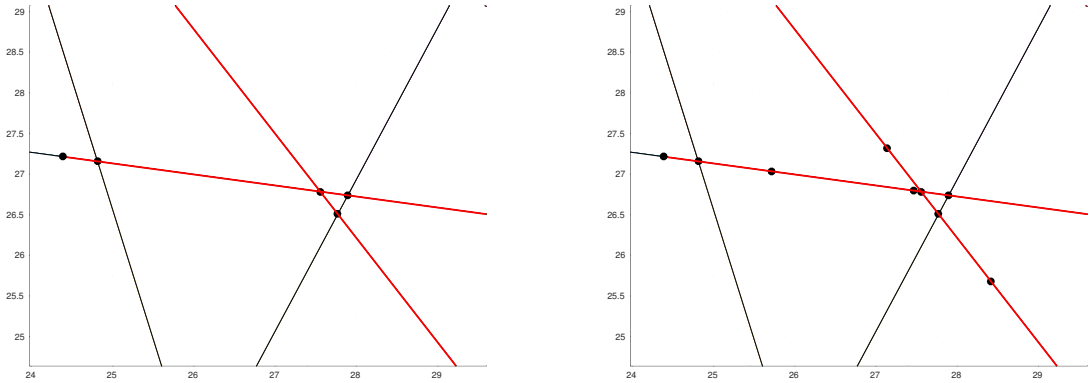

(a) Locally conforming mesh $\mathcal{T}_\delta^{\text{lc}}$ (b) Globally conforming mesh $\mathcal{T}_\delta^{\text{gc}}$

Figure 6: Details of the vertices of the discretizations on a trace

for the VEM approximation, and let E be a generic polygonal element of the mesh $\mathcal{T}^\star_{\delta i}$ for $i \in \mathcal{I}$ and $\star =' lc'$ or $'gc'$, as in subsection 4.1. Let us define on E the discrete functional space

$$V^E_{\delta i} := \left\{ v \in \mathrm{H}^1(E) : \gamma_e(v) \in \mathbb{P}_k(e) \ \forall e \subset \partial E,\ \Delta v|_E \in \mathbb{P}_{k-2}(E) \right\}, \tag{5}$$

and, on each fracture F_i the space

$$V^\star_{\delta i} := \left\{ v_\delta \in \mathbb{C}^0(F_i) : v \in V^E_{\delta i} \quad \forall E \in \mathcal{T}^\star_{\delta i} \right\}.$$

Then the discrete subspace of V with the VEM is:

$$V^\star_\delta := \left\{ v_\delta \in V : v \in V^\star_{\delta i} \quad \forall i \in \mathcal{I} \right\}, \tag{6}$$

spanned by basis functions $\phi^\star_\ell$, $\ell = 1, \dots, N_\ell$, being N_ℓ its dimension. The following set of degrees of freedom (DOFs) is introduced to uniquely define a function $v_\delta \in V^\star_{\delta i}$ [4]:

- the values of v_δ at each vertex in $\mathcal{V}^\star_\delta$;

and, if $k > 1$ also

- the values of v_δ at $k-1$ internal points (e.g. internal Gauss-Lobatto quadrature nodes) on each edge $e \in \mathcal{E}^\star_\delta$;
- the moments $\frac{1}{|E|}\int_E v_h m_{\boldsymbol{\alpha}}$ where $\boldsymbol{\alpha} = (\alpha_1, \alpha_2) \in \mathbb{N}^2$,

$$m_{\boldsymbol{\alpha}}(x, y) := \left(\frac{x - x_E}{h_E} \right)^{\alpha_1} \left(\frac{y - y_E}{h_E} \right)^{\alpha_2},$$

  $\forall E \in \mathcal{T}^\star_\delta$ and $\forall \boldsymbol{\alpha}$ such that $|\,\boldsymbol{\alpha}\,| \leq k-2$,

where (x_E, y_E) and h_E are the barycenter and the diameter of the element E, respectively. The chosen basis functions for $V^\star_\delta$ are Lagrangian with respect to this set of DOFs. We remark that functions ϕ_ℓ are not explicitly known in the interior of each element.

Assuming that the fracture transmissivity K_i is a constant function on each fracture, we introduce, for each $i \in \mathcal{I}$ and $E \in \mathcal{T}^\star_{\delta i}$, the operator $\Pi^\nabla_E \colon V^E_{\delta i} \to \mathbb{P}_k(E)$ defined as follows:

$$\begin{cases} \left(\mathrm{K}_i \nabla \Pi^\nabla_E \phi, \nabla p\right)_E = \left(\mathrm{K}_i \nabla \phi, \nabla p\right)_E & \forall p \in \mathbb{P}_k(E), \\ \sum_{V \in \mathcal{V}^{\mathrm{E}}_{\delta i}} \Pi^\nabla_E \phi(V) = \sum_{V \in \mathcal{V}^{\mathrm{E}}_{\delta i}} \phi(V) & \text{if } k = 1, \\ \int_E \Pi^\nabla_{E,k} v_\delta = \int_E v_\delta & \text{if } k > 1. \end{cases}$$

that can be computed by means of the above listed degrees of freedom, and the symmetric bilinear form $S^E \colon V^E_{\delta i} \times V^E_{\delta i} \to \mathbb{R}$, such that $\ker S^E \cap \ker \Pi^\nabla_E = \{0\}$ and

$$c_* \left(\mathrm{K}_i \nabla \phi, \nabla \phi\right)_E \leq S^E(\phi, \phi) \leq c^* \left(\mathrm{K}_i \nabla \phi, \nabla \phi\right)_E, \quad \forall \phi \in V^E_{\delta i},\ \text{s.t. } \Pi^\nabla_E \phi = 0 \tag{7}$$

for two positive constants c_* and c^*, independent of E and of the fracture F_i. The discrete counterpart of the bilinear form $a_i : V_i \times V_i \to \mathbb{R}$ in equation (1) is $a_{\delta i} \colon V^\star_{\delta i} \times V^\star_{\delta i} \to \mathbb{R}$, defined by

$$a_{\delta i}(v, w) := \sum_{E \in \mathcal{T}_{\delta i}} a^E_\delta(v, w),$$

where $a_\delta^E \colon V_\delta^\star \times V_\delta^\star \to \mathbb{R}$ is such that $\forall v, w \in V_\delta^\star$,

$$a_\delta^E(v,w) := \left(\mathrm{K}_i \nabla \Pi_E^\nabla v, \nabla \Pi_E^\nabla w\right)_E + S^E\left(v - \Pi_E^\nabla v, w - \Pi_E^\nabla w\right) .$$

Thanks to the definition of S^E and to property (7), the coercivity of the discrete bilinear form can be easily proven and it can be shown that it scales like $(\mathrm{K}_i \nabla v, \nabla v)_{F_i}$, i.e.:

$$\exists \alpha_*, \alpha^* > 0 \colon \alpha_* \left(\mathrm{K}_i \nabla v, \nabla v\right)_{F_i} \le a_{\delta i}(v,v) \le \alpha^* \left(\mathrm{K}_i \nabla v, \nabla v\right)_{F_i} . \tag{8}$$

For the computation of the discrete counterpart of the scalar product (f, v_δ) at the right-hand-side of equation (1), when v_δ is a function of the VEM space not known in the interior of each mesh element, we introduce the following discrete scalar product

$$(f_i, v_{\delta i})_{\delta, F_i} := \left(f_i, \tilde{\Pi}_k^0 v_{\delta i}\right)_{F_i} \quad \forall i \in \mathcal{I} ,$$

where the pseudo-projection $\tilde{\Pi}_k^0 : V_{\delta i} \to \mathbb{P}_k$ is defined, as in [3], by local projections, using $\Pi_{E,k}^\nabla v_{\delta i}$ in place of $v_{\delta i}$ to compute the moments of order $k-1$ and k:

$$\forall E \in \mathcal{T}_{\delta i}, \begin{cases} \left(\tilde{\Pi}_k^0 v_{\delta i}, p\right)_E = (v_{\delta i}, p)_E & \forall p \in \mathbb{P}_{k-2}(E) , \\ \left(\tilde{\Pi}_k^0 v_{\delta i}, p\right)_E = \left(\Pi_{E,k}^\nabla v_{\delta i}, p\right)_E & \forall p \in \mathbb{P}_k(E) \setminus \mathbb{P}_{k-2}(E) . \end{cases}$$

We finally introduce the following global discrete operators:

$$a_\delta(v,w) := \sum_{i \in \mathcal{I}} a_{\delta i}(v,w) \qquad \forall v, w \in V_\delta^\star,$$

$$(f, v_\delta)_\delta := \sum_{i \in \mathcal{I}} (f_i, v_{\delta i})_{\delta, F_i} \qquad \forall v \in V_\delta^\star.$$

Remark. A possible choice for the term S^E in the context of the simulation of the flow in DFNs is proposed in [9] and is given by the scalar product between the vectors containing the degrees of freedom of the two arguments on the element ([4, 6]). This choice guarantees property (7) under some basic regularity assumptions on the triangulation.

4.3 The locally conforming approach with Hybrid Mortar Virtual Elements

Let us now consider the locally conforming mesh $\mathcal{T}_\delta^{\mathrm{lc}}$ defined in subsection 4.1. Following [8], we will use the mortar method [11, 7, 12] to weakly enforce continuity of the solution h_δ across the traces. Let $m \in \mathcal{M}$ be a trace index and let i be the fracture index such that $(i,j) = \mathcal{I}_m$, we construct a discretization of Γ_m induced by the nodes of $\mathcal{T}_{\delta i}^{\mathrm{lc}}$, i.e. the nodes on Γ_m coincide with the vertices of the elements in $\mathcal{T}_{\delta i}^{\mathrm{lc}}$ lying on Γ_m. On this mesh the finite dimensional space $M_{\delta m}^{\mathrm{lc}} \subset \mathrm{L}^2(\Gamma_m)$ is defined, and we also set $M_\delta^{\mathrm{lc}} = \prod_{m \in \mathcal{M}} M_{\delta m}^{\mathrm{lc}}$. In the present context the space $M_{\delta m}^{\mathrm{lc}}$ contains piecewise (discontinuous) polynomials of degree k^λ in the interior of the trace and the polynomial functions of degree $k^\lambda - 1$ on the first and last intervals of the discretization, [11, 33, 8]. The discrete version of problem (3) within this framework is: find $h_\delta = h_\delta^0 + \mathcal{R}_\delta\left(h^D\right)$, with $h_\delta^0 \in V_\delta^{\mathrm{lc}}$ and $\lambda_\delta \in M_\delta^{\mathrm{lc}}$ such that,

$$\begin{cases} a_\delta\left(h_\delta^0, v_\delta\right) + b\left(v_\delta, \lambda_\delta\right) = (f, v_\delta)_\delta + \left(h^N, v_\delta\right)_{\Gamma^N} \\ \qquad\qquad - a_\delta\left(\mathcal{R}_\delta\left(h^D\right), v_\delta\right) & \forall v_\delta \in V_\delta^{\mathrm{lc}} , \\ b\left(h_\delta^0, \psi_\delta\right) = -b\left(\mathcal{R}_\delta\left(h^D\right), \psi_\delta\right) & \forall \psi_\delta \in M_\delta^{\mathrm{lc}} , \end{cases} \tag{9}$$

where the bilinear form $b(.,.)$ on each trace is evaluated as an $\mathrm{L}^2(\Gamma_m)$ scalar product.

Well posedness of (9) is proven in [8] under a quite common regularity assumption on the mesh. As a consequence the following *inf-sup* condition holds:

$$\inf_{\psi_\delta \in M_\delta^{\mathrm{lc}}} \sup_{v_\delta \in V_\delta^{\mathrm{lc}}} \frac{b(v_\delta, \psi_\delta)}{\|v_\delta\|_{V_\delta^{\mathrm{lc}}} \|\psi_\delta\|_{M_\delta^{\mathrm{lc}}}} \geq \beta\,,$$

for a constant $\beta > 0$ independent of δ. We remark that, in the present context the solution $\lambda_{\delta m}$ represents a piecewise polynomial approximation of $\left[\!\left[\frac{\partial h_i}{\partial \hat{n}_m^i}\right]\!\right]_{\Gamma_m}$. If we collect the DOFs for h_δ^0 and λ_δ in the vectors $\mathbf{h} \in \mathbb{R}^{N_h^{\mathrm{lc}}}$ and $\boldsymbol{\lambda} \in \mathbb{R}^{N_\lambda^{\mathrm{lc}}}$, respectively, the discrete solution is obtained solving the following linear system:

$$\begin{pmatrix} A & B^T \\ B & 0 \end{pmatrix} \begin{pmatrix} \mathbf{h} \\ \boldsymbol{\lambda} \end{pmatrix} = \begin{pmatrix} \mathbf{f} \\ \mathbf{d} \end{pmatrix},$$

where $A \in \mathbb{R}^{N_h^{\mathrm{lc}} \times N_h^{\mathrm{lc}}}$ is the block-diagonal matrix of the fracture-local stiffness matrices

$$(A_i)_{kl} = a_{\delta i}\left(\phi_{ki}^{\mathrm{lc}}, \phi_{li}^{\mathrm{lc}}\right).$$

The matrix $B \in \mathbb{R}^{N_\lambda^{\mathrm{lc}} \times N_h^{\mathrm{lc}}}$ collects the terms of the form:

$$B_{lk} := b\left(\phi_k^{\mathrm{lc}}, \mu_l^{\mathrm{lc}}\right) \quad \forall l \in \{1, \ldots, N_\lambda^{\mathrm{lc}}\},\, k \in \{1, \ldots, N_h^{\mathrm{lc}}\},$$

being ϕ_k^{lc} the k-th basis function of V_δ^{lc} and μ_l^{lc} the l-th basis function of M_δ^{lc}. Finally we have

$$\begin{aligned} f_k &:= \left(f, \phi_k^{\mathrm{lc}}\right)_\delta + \left(h^N, \phi_k^{\mathrm{lc}}\right)_{\Gamma^N} - a_\delta\left(\mathcal{R}_\delta\left(h^D\right), \phi_l^{\mathrm{lc}}\right) && \forall k \in \{1, \ldots, N_h^{\mathrm{lc}}\}, \\ d_l &:= -b\left(\mathcal{R}_\delta\left(h^D\right), \mu_l^{\mathrm{lc}}\right) && \forall l \in \{1, \ldots, N_\lambda^{\mathrm{lc}}\}. \end{aligned}$$

4.4 A globally conforming approach

A second approach, based on a globally conforming discretization of the DFN is proposed in in [10], where the matching conditions at the traces are strongly enforced by means of Lagrange multipliers. We set, on each fracture F_i, $i \in \mathcal{I}$, and on each trace Γ_m, $m \in \mathcal{M}_i$, the discretization induced by $\mathcal{T}_{\delta i}^{\mathrm{gc}}$, excluding the two extreme points (tips) of the trace, and we build, on this mesh the finite dimensional space

$$M_{\delta m,i}^{\mathrm{gc}} = \mathrm{span}\left\{\mu_{ki}^m,\ k = 1, \ldots, N_{\Gamma_m}^{\mathrm{gc}}\right\},$$

where $N_{\Gamma_m}^{\mathrm{gc}}$ is the number of interior nodes on Γ_m and μ_{ki}^m is a continuous linear operator such that

$$\left\langle \mu_{ki}^m, \gamma_{\Gamma_m}(v_{\delta j}) \right\rangle_{\Gamma_m} = \delta_{ij} v_{\delta i}(\mathbf{x}_k^m) \quad \forall v_\delta \in V_\delta^{\mathrm{gc}}, \tag{10}$$

being δ_{ij} the Kroneker delta and $\mathbf{x}_k^m$ the k-th node on trace Γ_m. We then set

$$M_{\delta m}^{\mathrm{gc}} := \left\{\mu_k^m \colon \mu_k^m = \mu_{ki}^m - \mu_{kj}^m \text{ if } \mathcal{I}_m = (i,j),\ k = 1, \ldots, N_{\Gamma_m}^{\mathrm{gc}}\right\},$$

and the discrete subspace $M_\delta^{\mathrm{gc}} \subset M$ is $M_\delta^{\mathrm{gc}} = \prod_{m \in \mathcal{M}} M_{\delta m}^{\mathrm{gc}}$. Observe that the continuity of functions $v_\delta \in V_\delta^\star$ across al the traces, i.e. the condition $[\![v_\delta]\!]_{\mathcal{M}} = 0$, is equivalent to an orthogonality condition of jumps across the traces with respect to the space M_δ^{gc}

$$b(v_\delta, \psi_\delta) = 0 \quad \forall \psi_\delta \in M_\delta^{\mathrm{gc}} \iff [\![v_\delta]\!]_{\mathcal{M}} = 0\,,$$

being for any $m \in \mathcal{M}$, if $\mathcal{I}_m = (i,j)$, $\forall k \in \{1,\dots,N^{\mathrm{gc}}_{\Gamma_m}\}$,

$$\left\langle \mu^m_k, [\![v_\delta]\!]_{\Gamma_m} \right\rangle_{\Gamma_m} = \left\langle \mu^m_{ki}, \gamma_{\Gamma_m}(v_{\delta i}) \right\rangle_{\Gamma_m} - \left\langle \mu^m_{kj}, \gamma_{\Gamma_m}(v_{\delta j}) \right\rangle_{\Gamma_m} = v_{\delta i}(\mathbf{x}^m_k) - v_{\delta j}(\mathbf{x}^m_k).$$

Setting $h_\delta = h^0_\delta + \mathcal{R}_\delta\left(h^D\right)$, with $h^0_\delta \in V^{\mathrm{gc}}_\delta$ and $\mathcal{R}_\delta\left(h^D\right)$ the lifting of the boundary conditions, the discrete solution to (3) $(h^0_\delta, \lambda_\delta) \in V^{\mathrm{gc}}_\delta \times M^{\mathrm{gc}}_\delta$, such that

$$\mathcal{F}\left(h^0_\delta, \lambda_\delta\right) = \min_{v_\delta \in V^{\mathrm{gc}}_\delta} \max_{\psi_\delta \in M^{\mathrm{gc}}_\delta} \mathcal{F}(v_\delta, \psi_\delta) \ ,$$

is given by the solution of:

$$\begin{cases} a_\delta\left(h^0_\delta, v_\delta\right) + b\left(v_\delta, \lambda_\delta\right) = (f, v_\delta)_\delta + \left\langle h^N, \gamma_{\Gamma^N}(v_\delta)\right\rangle_{\Gamma^N} \\ \qquad\qquad\qquad\qquad + a_\delta\left(\mathcal{R}_\delta\left(h^D\right), v_\delta\right) & \forall v_\delta \in V^{\mathrm{gc}}_\delta, \\ b\left(h^0_\delta, \psi_\delta\right) = -b\left(\mathcal{R}_\delta\left(h^D\right), \psi_\delta\right) & \forall \psi_\delta \in M^{\mathrm{gc}}_\delta. \end{cases}$$

This problem is well posed, as it can be easily proven, observing that, given the space

$$W^{\mathrm{gc}}_\delta := \{v_\delta \in V^{\mathrm{gc}}_\delta \colon b(v_\delta, \psi_\delta) = 0 \quad \forall \psi_\delta \in M^{\mathrm{gc}}_\delta\} = \left\{v_\delta \in V^{\mathrm{gc}}_\delta \colon [\![v_\delta]\!]_{\Gamma_m} = 0 \quad \forall m \in \mathcal{M}\right\} \ ,$$

$v_\delta \mapsto \sum_{i\in\mathcal{I}} (\mathrm{K}_i \nabla v_{\delta i}, \nabla v_{\delta i})_{F_i}$ is a norm on W^{gc}_δ and then a_δ is coercive on W^{gc}_δ thanks to (8), and to the fact that

$$\forall \psi_\delta \in M^{\mathrm{gc}}_\delta, \quad \sup_{v_\delta \in V^{\mathrm{gc}}_\delta} \frac{b(v_\delta, \psi_\delta)}{\|v_\delta\|_{V^{\mathrm{gc}}_\delta}} = \|\psi_\delta\|_{M^{\mathrm{gc}}_\delta} \ .$$

The discrete solution in the present framework can be obtained solving the linear system

$$\begin{pmatrix} A & B^T \\ B & 0 \end{pmatrix} \begin{pmatrix} \mathbf{h} \\ \boldsymbol{\lambda} \end{pmatrix} = \begin{pmatrix} \mathbf{f} \\ \mathbf{d} \end{pmatrix} \ , \tag{11}$$

where $\mathbf{h}$ is the vector collecting all the DOFs for h_δ, $\boldsymbol{\lambda}$ is the vector of Lagrange multipliers, $\mathbf{f}$ is the vector containing the right-hand-side terms, $\mathbf{d}$ the vector of nodal values of h^D on the traces. Matrix A is again the block diagonal matrix obtained collecting the stiffness matrices A_i related to the VEM discrete bilinear forms on the globally conforming mesh of each fracture:

$$(A_i)_{kl} = a_{\delta i}\left(\phi^{\mathrm{gc}}_{ki}, \phi^{\mathrm{gc}}_{li}\right) \ .$$

Matrix B is related to the bilinear form $b(v_\delta, \psi_\delta)$ in the following way. Let us observe that

$$b_i\left(\phi^{\mathrm{gc}}_l, \mu^m_k\right) = \begin{cases} (-1)^{s_{\Gamma_m}(i)} & \text{if } \mathbf{x}_l = \mathbf{x}^m_k, \\ 0 & \text{otherwise,} \end{cases}$$

where $\mathbf{x}_l$ are the coordinates of the mesh vertex such that $\phi_l(\mathbf{x}_l) = 1$. After introducing a global numbering for the degrees of freedom on all the traces according to trace numbering, we introduce, for each trace index $m \in \mathcal{M}$, the row vector B_m such that $(B_m)_k = 1$ if $\mu^m_k \in M^{\mathrm{gc}}_{\delta m,i}$ and $(B_m)_k = -1$ if $\mu^m_k \in M^{\mathrm{gc}}_{\delta m,j}$ with $(i,j) = \mathcal{I}_m$. Finally

$$B := \begin{pmatrix} B_1 \\ \vdots \\ B_M \end{pmatrix} \ .$$

The solution to (11) is unique, as it can be proven using classical results (see e.g. [28]). Further, within this framework it is possible to use preconditioning techniques borrowed from domain decomposition method, as for example the one-level FETI preconditioner [25], as shown in [10].

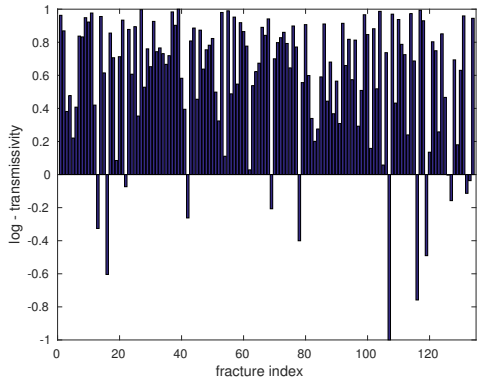

(a) Values of the transmissivity on each fracture (the vertical axis is in log-scale).

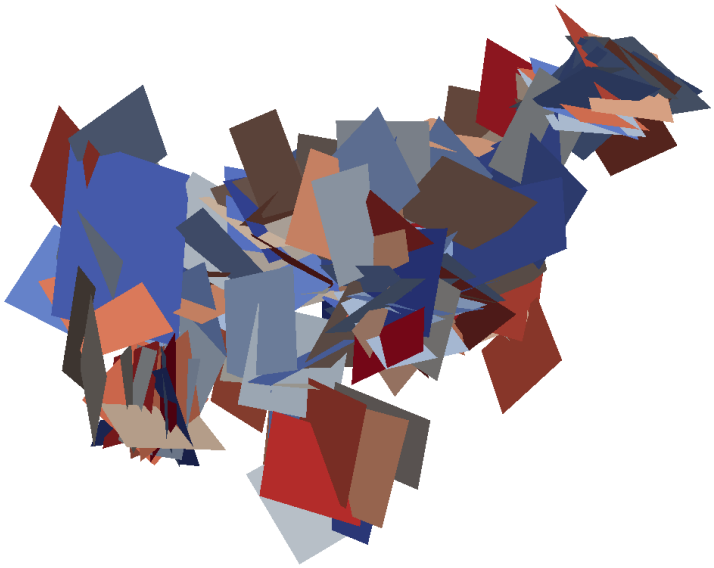

(b) Plot of the distribution of transmissivity.

Figure 7: The distribution of transmissivity chosen for the numerical test.

5 Numerical results

For numerical results about the convergence behaviour of the described methods we refer the reader to [10, 8]. Here we focus on the application of the globally conforming method and the VEM-Mortar approach to a almost realistic DFN.

Let us consider the 134 Fractures DFN already depicted in Figure 1. We impose a non-null Neumann boundary condition (an incoming flux) on one side of three source fractures, a homogeneous Dirichlet boundary condition on one side of a sink fracture, and a homogeneous Neumann boundary condition (no flux) on all other boundaries. The forcing term is the null function, i.e. we assume there are no internal sources or sinks inside the fractures; this corresponds to neglect the effect on the fractures of the surrounding rock matrix. We assume a constant transmissivity on each fracture, with values randomly distributed between 10^{-1} and 10, displayed in Figure 7a. As we can see in Figure 7b, there are significant jumps of transmissivity between intersecting fractures. See Figure 8 for the discrete hydraulic head obtained with the globally conforming method and Figure 10 for a visualization of the solutions obtained by the two methods using the same base mesh, on two particular fractures.

In practical applications, the most important quantity to be evaluated is the flux through the traces. This is obtained as a direct solution (the Lagrange multiplier) of the system if the VEM-Mortar method is used, whereas in the globally conforming case it has to be computed as a post-processing of the discrete VEM solution, first projecting the latter on the space of polynomials of degree k and then computing the jump of the co-normal derivative of the projection in correspondence of traces.

The two considered approaches yield very similar results, as we can see in Figure 9, where we show the discrete fluxes computed with VEM of order 1 and the results for the VEM-Mortar method are obtained using continuous piecewise linear Lagrange multipliers. We remark that the oscillations of the discrete flux coming from the Mortar approach are justified by the fact that convergence is proved in the $\mathrm{H}^{-\frac{1}{2}}(\Gamma_m)$ norm, $\forall m \in \mathcal{M}$, which is a weaker norm than the $\mathrm{L}^2(\Gamma_m)$ norm.

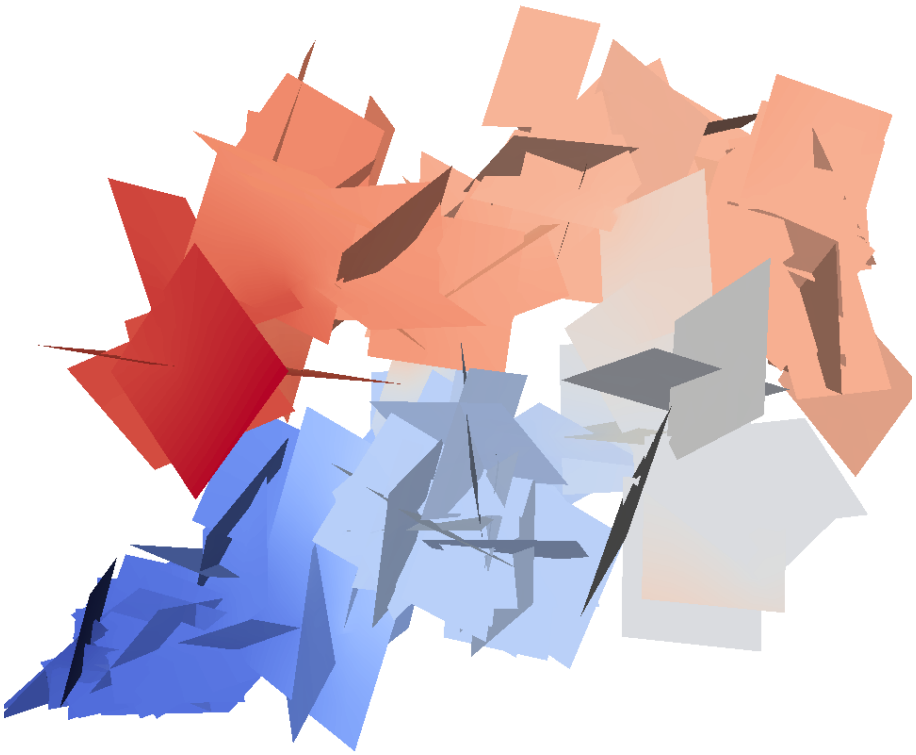

Figure 8: A discrete solution of the problem.

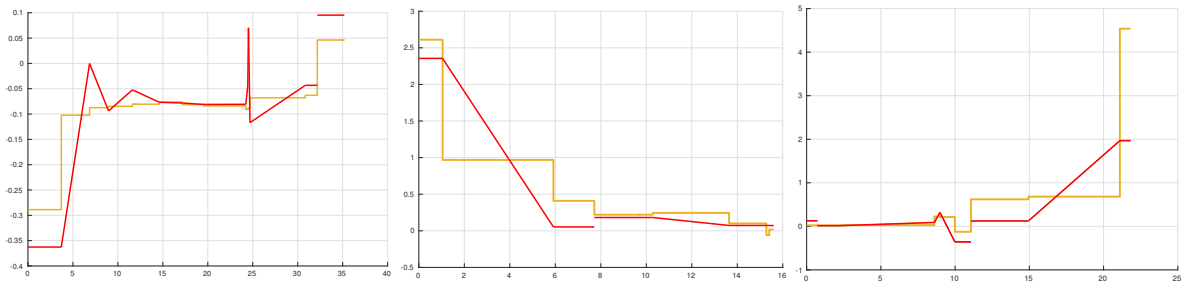

Figure 9: Comparison of fluxes computed by the two methods on three selected traces. Yellow: globally conforming VEM. Red: VEM-Mortar.

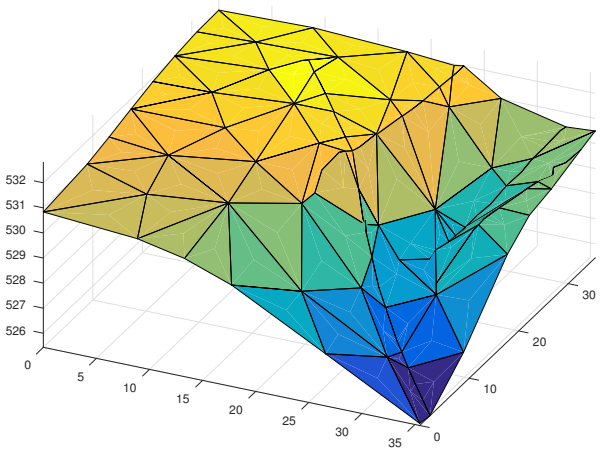

(a) Globally conforming method

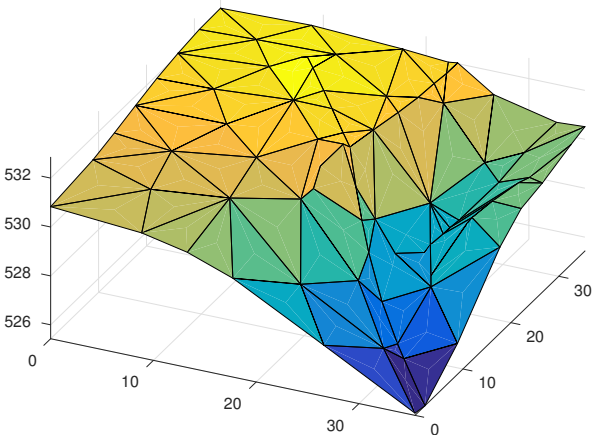

(b) VEM-Mortar method

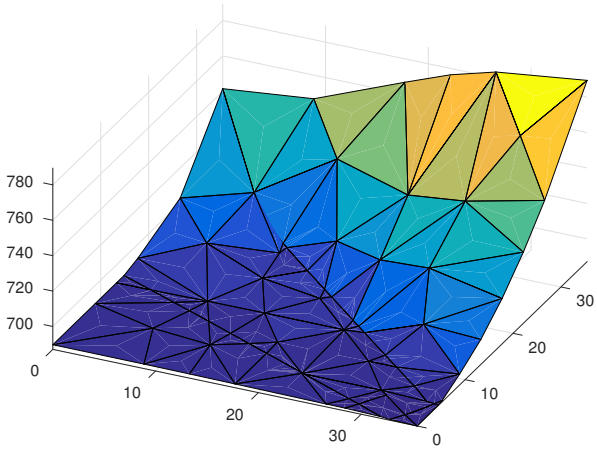

(c) Globally conforming method

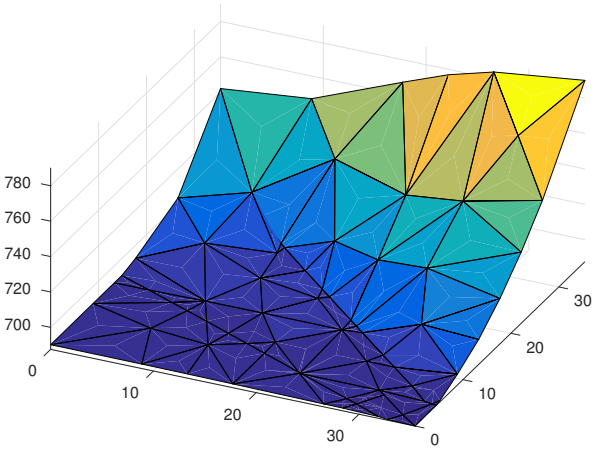

(d) VEM – Mortar method

Figure 10: Solutions given by the two approaches on two selected fractures

6 Conclusions

We have shown that the capability of the VEM to handle a large class of polygons enables to easily construct functional spaces defined on local meshes on each of the fractures that are locally or globally conforming to traces. This allows for the use of standard domain decomposition approaches, coupling local problems by a Mortar method or, if meshes are globally conforming, by resorting to global continuity. Numerical results on the computed discrete fluxes at traces show that the two approaches are viable and sufficiently relaibale.

7 Acknowledgement

This work has been supported by the Italian MIUR through PRIN research grant 2012HBLYE4_001 "Metodologie innovative nella modellistica differenziale numerica" and by INdAM-GNCS.

Fernando Matìas Benedetto was supported by the European Commission through the Erasmus Mundus Action 2-Strand1 ARCOIRIS programme, Politecnico di Torino.

Stefano Berrone also acknowledges the partial financial support received from the European Unions Seventh Framework Programme (FP7/ 20142016) under Grant Agreement Number 607626 (Safeciti). Project title: "Simulation Platform for the Analysis of Crowd Turmoil in Urban Environments with Training and Predictive Capabilities". This publication reflects the views only of the authors and the Commission cannot be held responsible for any use which may be made of the information here contained.

REFERENCES

[1] P. M. Adler. *Fractures and Fracture Networks*. Kluwer Academic, Dordrecht, 1999.

[2] B. Ahmad, A. Alsaedi, F. Brezzi, L. D. Marini, and A. Russo. Equivalent projectors for virtual element methods. *Comput. Math. Appl.*, 66(3):376–391, September 2013.

[3] F. Beirão da Veiga, L. Brezzi, L. D. Marini, and A. Russo. The hitchhikers guide to the virtual element method. *Mathematical Models and Methods in Applied Sciences*, 24(08):1541–1573, 2014.

[4] L. Beirão da Veiga, F. Brezzi, A. Cangiani, G. Manzini, L. D. Marini, and A. Russo. Basic principles of virtual element methods. *Math. Models Methods Appl. Sci.*, 23(1):199–214, 2013.

[5] L. Beirão da Veiga, F. Brezzi, and L. D. Marini. Virtual elements for linear elasticity problems. *SIAM J. Numer. Anal.*, 51(2):794–812, 2013.

[6] L. Beirão da Veiga, F. Brezzi, L. D. Marini, and A. Russo. Virtual element method for general second-order elliptic problems on polygonal meshes. *Mathematical Models and Methods in Applied Sciences*.

[7] F.B. Belgacem. The mortar finite element method with lagrange multipliers. *Numerische Mathematik*, 84(2):173–197, 1999.

[8] M.F. Benedetto, S. Berrone, A. Borio, S. Pieraccini, and S. Scialò. A hybrid mortar virtual element method for discrete fracture network simulations. *J. Comput. Phys.*, 306:148–166, 2016.

[9] M.F. Benedetto, S. Berrone, S. Pieraccini, and S. Scialò. The virtual element method for discrete fracture network simulations. *Comput. Methods Appl. Mech. Engrg.*, 280(0):135 – 156, 2014.

[10] M.F. Benedetto, S. Berrone, and S. Scialò. A globally conforming method for solving flow in discrete fracture networks using the virtual element method. *Finite Elem. Anal. Des.*, 109:23–36, 2016.

[11] C. Bernardi, Y. Maday, and A. T. Patera. A new nonconforming approach to domain decomposition: the mortar element method. In *Nonlinear partial differential equations and their applications. Collège de France Seminar, Vol. XI (Paris, 1989–1991)*, volume 299 of *Pitman Res. Notes Math. Ser.*, pages 13–51. Longman Sci. Tech., Harlow, 1994.

[12] C. Bernardi, Y. Maday, and F. Rapetti. Basics and some applications of the mortar element method. *GAMM-Mitt.*, 28(2):97–123, 2005.

[13] S. Berrone, A. Borio, and S. Scialò. A posteriori error estimate for a PDE-constrained optimization formulation for the flow in DFNs. *SIAM J. Numer. Anal.*, 54(1):242–261, 2016.

[14] S. Berrone, C. Canuto, S. Pieraccini, and S. Scialò. Uncertainty quantification in discrete fracture network models: stochastic fracture transmissivity. *Comput. Math. Appl.*, 70(4):603–623, 2015.

[15] S. Berrone, S. Pieraccini, and S. Scialò. A PDE-constrained optimization formulation for discrete fracture network flows. *SIAM J. Sci. Comput.*, 35(2):B487–B510, 2013.

[16] S. Berrone, S. Pieraccini, and S. Scialò. On simulations of discrete fracture network flows with an optimization-based extended finite element method. *SIAM J. Sci. Comput.*, 35(2):A908–A935, 2013.

[17] S. Berrone, S. Pieraccini, and S. Scialò. An optimization approach for large scale simulations of discrete fracture network flows. *J. Comput. Phys.*, 256:838–853, 2014.

[18] S. Berrone, S. Pieraccini, and S. Scialò. Towards effective flow simulations in realistic discrete fracture networks. *J. Comput. Phys.*, 310:181–201, 2016.

[19] S. Berrone, S. Pieraccini, S. Scialò, and F. Vicini. A parallel solver for large scale DFN flow simulations. *SIAM J. Sci. Comput.*, 37(3):C285–C306, 2015.

[20] D. Blessent, R. Therrien, and C.W. Gable. Large-scale numerical simulation of groundwater flow and solute transport in discretely-fractured crystalline bedrock. *Advances in Water Resources*, 34(12):1539 – 1552, 2011.

[21] F. Brezzi, R.S. Falk, and D.L. Marini. Basic principles of mixed virtual element methods. *ESAIM: Mathematical Modelling and Numerical Analysis*, 48(04):1227–1240, 2014.

[22] W. S. Dershowitz and C. Fidelibus. Derivation of equivalent pipe networks analogues for three-dimensional discrete fracture networks by the boundary element method. *Water Resource Res.*, 35:2685–2691, 1999.

[23] L. Formaggia, A. Fumagalli, A. Scotti, and P. Ruffo. A reduced model for Darcy's problem in networks of fractures. *ESAIM: Mathematical Modelling and Numerical Analysis*, 48:1089–1116, 7 2014.

[24] J.D. Hyman, C.W. Gable, S.L. Painter, and N. Makedonska. Conforming delaunay triangulation of stochastically generated three dimensional discrete fracture networks: A feature rejection algorithm for meshing strategy. *SIAM Journal on Scientific Computing*, 36:A1871–A1894, 2014.

[25] A. Klawonn. FETI domain decomposition methods for second order elliptic partial differential equations. *GAMM-Mitteilungen*, 29(2):319–341, 2006.

[26] D. Mora L. Beirão da Veiga, C. Lovadina. A virtual element method for elastic and inelastic problems on polytope meshes. *ArXiv*, 2015.

[27] V. Lenti and C. Fidelibus. A *bem* solution of steady-state flow problems in discrete fracture networks with minimization of core storage. *Computers & Geosciences*, 29(9):1183 – 1190, 2003.

[28] J. Nocedal and S.J. Wright. *Numerical Optimization*. Springer, Berlin, 1999.

[29] G. Pichot, J. Erhel, and J. de Dreuzy. A mixed hybrid mortar method for solving flow in discrete fracture networks. *Applicable Analysis*, 89:1629 – 643, 2010.

[30] G. Pichot, J. Erhel, and J. de Dreuzy. A generalized mixed hybrid mortar method for solving flow in stochastic discrete fracture networks. *SIAM Journal on scientific computing*, 34:B86 – B105, 2012.

[31] P.A. Raviart and J.M. Thomas. Primal hybrid finite element methods for 2nd order elliptic equations. *Mathematics of computation*, 31(138):391–413, 1977.

[32] M. Vohralík, J. Maryška, and O. Severýn. Mixed and nonconforming finite element methods on a system of polygons. *Applied Numerical Mathematics*, 51:176–193, 2007.

[33] B.I. Wohlmuth. A mortar finite element method using dual spaces for the lagrange multiplier. *SIAM journal on numerical analysis*, 38(3):989–1012, 2000.